



# Precipitate coarsening parameters for gas induced semi-solid cast 7075-T6 Al alloy determined by SAXS measurements

N MAHATHANINWONG<sup>1,\*</sup>, S WISUTMETHANGOON<sup>2</sup>, T CHUCHEEP<sup>1</sup>, S JANUDOM<sup>3</sup> and R CANYOOK<sup>4</sup>

<sup>1</sup>Faculty of Science and Industrial Technology, Prince of Songkla University, Surat Thani Campus, Muang, Surat Thani 84000, Thailand

<sup>2</sup>Department of Mechanical Engineering, Faculty of Engineering, Prince of Songkla University, Hat Yai, Songkhla 90112, Thailand

<sup>3</sup>Department of Mining and Materials Engineering, Faculty of Engineering, Prince of Songkla University, Hat Yai, Songkhla 90112, Thailand

<sup>4</sup>Department of Materials and Production of Technology Engineering, Faculty of Engineering, King Mongkut's University of Technology North Bangkok, Bangkok 10800, Thailand

\*Author for correspondence (narissara.s@psu.ac.th)

MS received 3 August 2016; accepted 27 March 2017; published online 31 October 2017

**Abstract.** The particle radii of precipitates in the gas induced semi-solid (GISS) cast 7075-T6 Al alloys, for ageing times ranging from peak ageing to over ageing, were measured by small-angle X-ray scattering (SAXS) technique. The measured precipitate radii increased with ageing time and temperature, and data were well fit by the Lifshitz–Slyozov–Wagner (LSW) coarsening process along with a modified Arrhenius equation for temperature dependency. The activation energy for the coarsening process was estimated at 1.19 eV, which is close to that of the wrought 7075 Al alloy. This energy is in the range of activation energies of Zn, Mg and Cu for their diffusion in Al. The precipitate coarsening rate of this alloy appears to be diffusion limited. The fine precipitates of the GISS 7075-PA Al alloy coarsened slowly at  $63 \text{ nm}^3 \text{ h}^{-1}$  rate, at the elevated  $200^\circ\text{C}$  temperature, while rapid  $216 \text{ nm}^3 \text{ h}^{-1}$  coarsening was found in the wrought 7075-T651 Al alloy.

**Keywords.** 7075 Al alloy; gas induced semi-solid; small angle X-ray scattering; precipitate coarsening.

## 1. Introduction

Mechanical properties of the wrought 7075 Al alloy are superior to those of other Al alloys. This is a precipitate hardening alloy [1]. Precipitates of the alloy after ageing have been analysed to gain understanding of the precipitate hardening mechanisms. Such information on various wrought 7xxx Al alloys is available especially on the wrought 7075 Al alloy [2,3]. Previous work [4] was reported on the peak aged condition of the cast 7075 Al alloy, which was produced by semi-solid forming process through gas induced semi-solid (GISS) technique. Precipitates at peak aged and onset hardness plateau times of the alloy were also characterized by transmission electron microscope (TEM). The tensile strength of GISS 7075-T6 was found to be comparable to that of some thixo-formed products but lower than that of wrought 7075-T651. However, surprisingly its creep resistance was superior to wrought 7075-T651 [5]. Hence, it is of interest to study the behaviour of precipitate coarsening in the GISS processed 7075-T6 Al alloy in order to figure out the potential for using this alloy at elevated temperatures and surpassing the properties of the wrought 7075 Al alloy.

This work will further investigate the precipitate evolution of the alloy aged at 120, 145, 165 and  $185^\circ\text{C}$  for various times after peak ageing and onset of hardness plateau times. The influence of ageing temperature and time on the precipitate evolution of the alloy was investigated, mainly by small angle X-ray scattering (SAXS), to gain a better understanding of the precipitate coarsening mechanisms in the alloy. Furthermore, the precipitate coarsening was determined as well, for both the GISS 7075-T6 PA and the wrought 7075-T651 Al alloy, at the elevated  $200^\circ\text{C}$  temperature.

## 2. Experimental

The semi-solid cast 7075 Al alloy was prepared through the GISS process, as detailed in the previous work [4]. The wrought 7075 Al alloy used in the present work was received as 12.7-mm-thick rolled plates in the T651 condition, to be used in comparisons. The chemical compositions of the alloys are shown in table 1 and were determined by optical emission spectroscopy.

The as-cast plates were cut into small  $15 \times 50 \times 15 \text{ mm}$  samples and subjected to T6 heat treatment. These samples

**Table 1.** Chemical composition of the GISS cast 7075-T6 Al alloy (GISS) and the wrought 7075 Al alloy (wrought) in wt%.

Element	Zn	Mg	Cu	Fe	Si	Cr	Mn	Al
GISS	6.08	2.50	1.93	0.46	0.40	0.19	0.03	Bal.
Wrought	5.92	2.64	1.70	0.19	0.07	0.19	0.04	Bal.

were solution heat treated at 450°C for 4 h, quenched in 25°C water, after that artificially aged at 120, 145, 165 and 185°C beyond the peak ageing time and the onset of the hardness plateau [4]. The GISS 7075-T6 Al alloy aged after peak age at 120°C for 72 h (GISS-PA), and the as-received wrought (AR-W) 7075-T651 Al alloy was heated at 200°C for 1 h or for 4 h.

To prepare TEM specimens, each specimen was machined into a 3-mm diameter rod inserted in wood. This rod was then sliced into approximately 0.8 mm thick discs using a low speed diamond saw. Both sides of the discs were mechanically polished with 1200-grit SiC and 5 µm micro-polishing alumina powder, leaving a 40–60 µm thick sample. These thin disc specimens were then electropolished in a Tenupol-3 electropolisher, with a solution of 20–25 vol% nitric acid and 80–75 vol% methanol at –15 to –20°C and an applied current of 1.2–1.5 A. Each electropolished specimen was immersed into methanol for cleaning. The electropolished specimens

were then characterized using a JEM-2010 JEOL TEM at MTEC.

The SAXS specimens were thin sheets cut from these aged samples with a 7 mm × 7 mm face and a 50–70 µm thickness. The proven quantitative analysis of precipitates in Al alloys by SAXS technique dates back to more than 30 years [6]. This study used the SAXS beamline of the Siam Photon Laboratory in the Synchrotron Light Research Institute (SLRI), Suranaree University of Technology, Thailand, which was opened for users in March 2011, as described in [7,8]. The incident X-rays had 8–9.5 keV energy and their scattering vector  $q$  was in the range from 0.1 to 2.5 nm<sup>-1</sup>, and the sample to detector distance was 1.2 and 4.5 m.

### 3. Results and discussion

#### 3.1 TEM micrographs

Figure 1a and b shows representative images of precipitate for the GISS 7075 Al alloy aged at 120°C for 72 h (peak ageing) and for 132 h (over ageing), respectively. The precipitates at their peak aged condition were finer and could not be quantified as mentioned in a previous study by Mahathaninwong *et al* [4]. The coarsening of precipitates was obvious when ageing time was extended to 132 h. Figure 1c shows the precipitate morphology of the specimen aged at 145°C for 6 h with the average diameter being 4.09 nm [4]. The precipitates

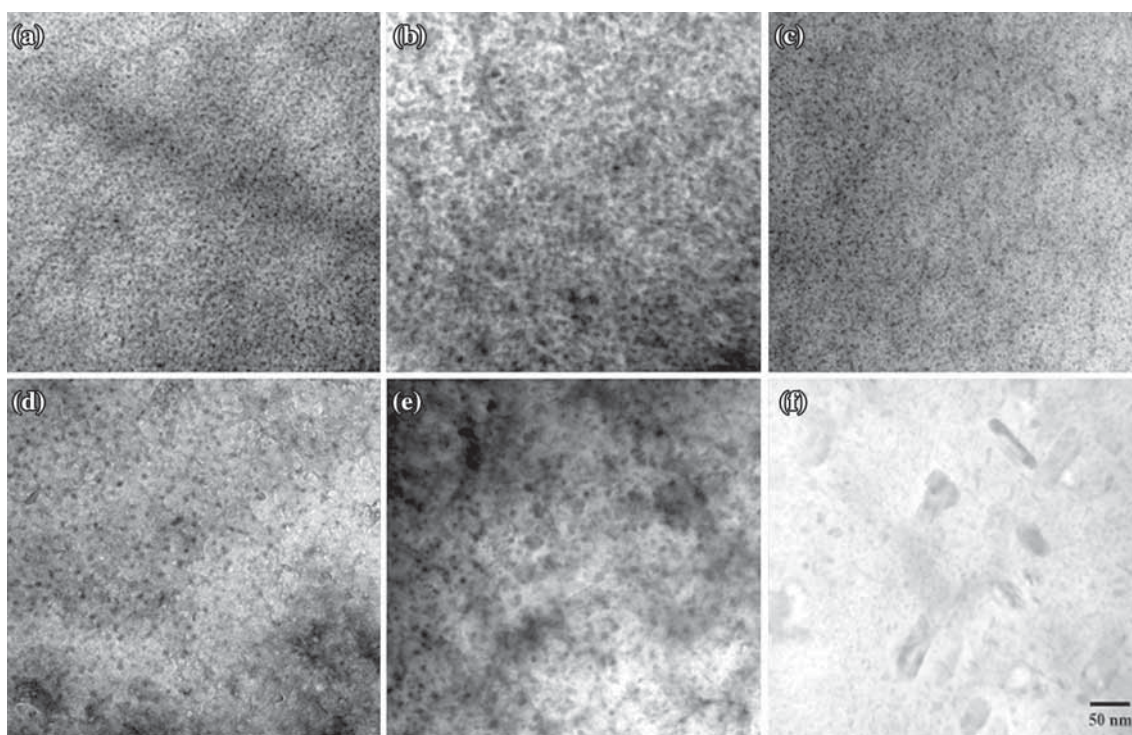


**Figure 1.** TEM micrographs of GISS cast 7075-T6 aged specimens at (a) 120°C for 72 h [4], (b) 120°C for 132 h, (c) 145°C for 6 h, (d) 145°C for 24 h, (e) 145°C for 72 h and of (f) as-received wrought 7075-T651 Al alloy.

became coarser with 24 and 72 h ageing times as shown in figure 1d and e, respectively. TEM images of specimens aged at 165°C for 3 h and at 185°C for 1 h have been shown in previous work [4].

It was reported in a previous study [5] that the creep resistance of GISS cast 7075-T6 Al alloy aged at 120°C for 72 h was superior to that of the wrought 7075 Al alloy, when observed at 200°C for stresses in the range 120–180 MPa. The precipitates of the wrought alloy before creep test are shown in figure 1f. Dense and fine precipitates prevailed in the microstructure of the GISS alloy as seen in figure 1a. Moreover, the precipitate size in the alloy is rather uniform. In contrast, large sized precipitates appeared alongside the fine precipitates in the microstructure of the wrought Al alloy. No quantitative analysis of these precipitates has been reported in prior studies. The quantitative characterization of both these alloys is investigated here with SAXS.

### 3.2 Small angle X-ray scattering

A SAXS data processing programme, SAXSIT (small angle X-ray scattering image tool) [9], was used to determine the Guinier (Gyration) radius ( $R_G$ ). Following the Guinier approximation, the scattered intensity can be written as given in equation (1) [6];

$$I(q) = I_e N n^2 e^{-R_G^2 q^2 / 3} \quad (1)$$

Where  $I(q)$  is the relative scattered intensity,  $I_e$  is the scattered intensity by one electron,  $n$  is the total electron count in one particle and  $N$  the total number of particles in the field irradiated by X-rays.  $R_G$  is calculated through the slope  $m$  in a Guinier plot of  $\ln I$  and  $q^2$ , with  $R_G = \sqrt{-3m}$ . An average radius ( $R$ ) of spherical and ellipsoidal precipitate particles can be estimated as shown below in equation (2);

$$R = \sqrt{\frac{5}{3}} R_G. \quad (2)$$

The scattering curves for the GISS-cast 7075-T6 specimens, aged in the range of 120–185°C temperatures for various times, are shown in figures 2 and 3 as semi-log plots of  $\log I$  vs.  $q^2$ . The scattering curves for GISS-cast 7075-T6 aged at 120°C for 1 h (GISS-PA) and wrought 7075-T651, heated at 200°C for 1 and 4 h, are shown in figures 4 and 5. The observations appear nearly linear over the small angle region. Therefore, the Guinier radii were calculated from the slopes observed in the range  $0.8 < q * R < 2$  [10], and the average  $R_G$  and  $R$  are summarized in table 2.

The average precipitate radius of peak aged specimen was consistent with that of 7150 Al alloy aged at 120°C for 24 h [11], while a finer 2.13 nm precipitate radius has been reported for the wrought 7075 Al alloy aged at 120°C for 72 h [2]. At each ageing temperature the average precipitate radius increased significantly with observed ageing times up to 72 h

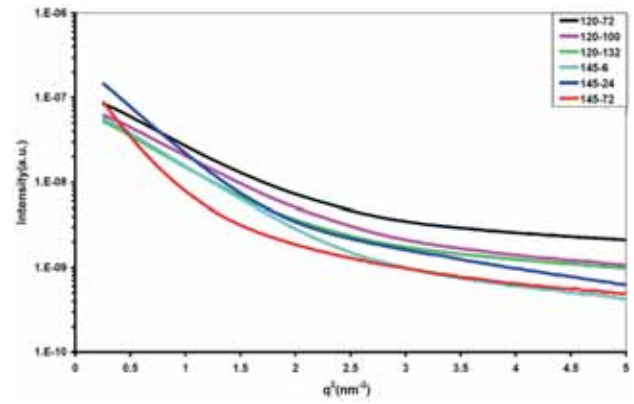


**Figure 2.** Guinier semi-log plots of  $I$  vs.  $q^2$  for the 7075-T6 Al alloy aged at 120°C for 72 h (120–72), 100 h (120–100) and 132 h (120–132); and at 145°C for 6 h (145–6), 24 h (145–24) and 72 h (145–72).

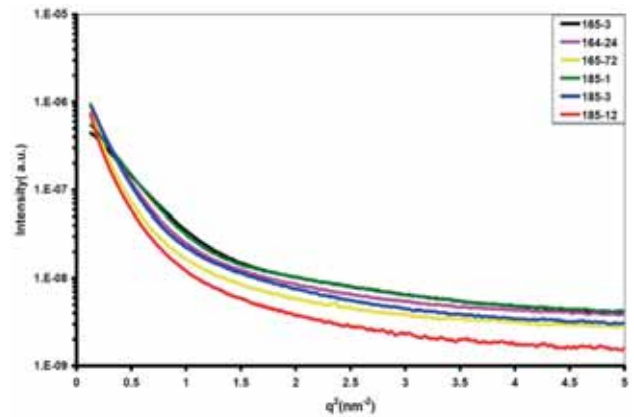


**Figure 3.** Guinier semi-log plots of  $I$  vs.  $q^2$  for the 7075-T6 Al alloy aged at 165°C for 3 h (165–3), 24 h (165–24) and 72 h (165–72); and at 185°C for 1 h (185–1), 3 h (185–3) and 12 h (185–12).

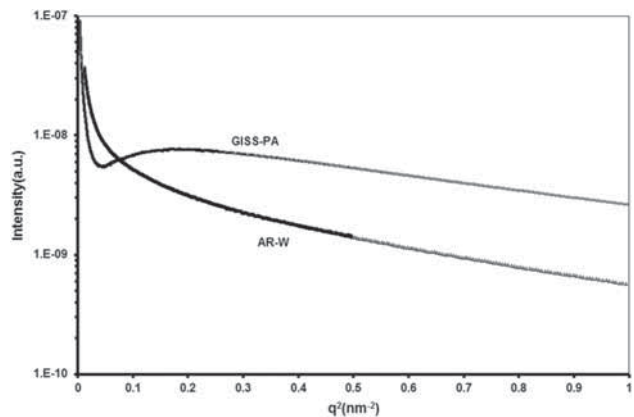


**Figure 4.** Guinier semi-log plots of  $I$  vs.  $q^2$  for the 7075-T6 Al alloy aged at 120°C for 72 h (GISS-PA) and for as-received wrought 7075-T651 Al alloy (AR-W).

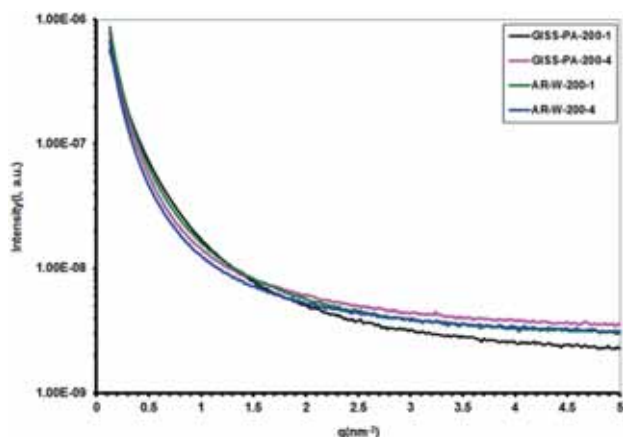


**Figure 5.** Guinier semi-log plots of  $I$  vs.  $q^2$  for the 7075-T6 PA heating at 200°C for 1 h (GISS-PA-200-1) and 4 h (GISS-PA-200-4) and as-received wrought 7075 Al alloy heating at 200°C for 1 h (AR-W-200-1) and 4 h (AR-W-200-4).

**Table 2.** The average Guinier radii and estimated precipitate radii of the GISS cast 7075-T6 and wrought 7075-T651 Al alloy for various conditions as determined from the SAXS curves.

Ageing treatments	$R_G$ (nm)	$R$ (nm)
120°C/72 h (120–72)	$2.09 \pm 0.16$	$2.50 \pm 0.21$
120°C/100 h (120–100)	$2.12 \pm 0.18$	$2.52 \pm 0.23$
120°C/132 h (120–132)	$2.22 \pm 0.19$	$2.69 \pm 0.25$
145°C/6 h (145–6)	$2.29 \pm 0.18$	$2.80 \pm 0.24$
145°C/24 h (145–24)	$2.68 \pm 0.05$	$3.46 \pm 0.06$
145°C/72 h (145–72)	$3.28 \pm 0.07$	$4.31 \pm 0.09$
165°C/3 h (165–3)	$2.98 \pm 0.04$	$3.91 \pm 0.06$
165°C/24 h (165–24)	$3.62 \pm 0.16$	$4.91 \pm 0.2$
165°C/72 h (165–72)	$4.07 \pm 0.38$	$5.66 \pm 0.49$
185°C/1 h (185–1)	$3.22 \pm 0.02$	$4.17 \pm 0.02$
185°C/3 h (185–3)	$3.85 \pm 0.17$	$5.20 \pm 0.21$
185°C/12 h (185–12)	$4.03 \pm 0.56$	$5.85 \pm 0.76$
GISS-PA-200-1	$3.35 \pm 0.47$	$4.32 \pm 0.61$
GISS-PA-200-4	$5.00 \pm 0.92$	$6.46 \pm 1.19$
AR-W	$3.1 \pm 0.31$	$4.00 \pm 0.40$
AR-W-200-1	$4.96 \pm 0.84$	$6.41 \pm 1.09$
AR-W-200-4	$7.55 \pm 2.10$	$9.75 \pm 2.72$

and similarly the radii consistently increased with the ageing temperature. The obtained average precipitate radii from SAXS measurements are known to be closely similar to those determined from TEM images [4].

However, the scattering intensity of GISS-cast 7075-T6 aged at 120°C for 72 h (GISS-PA) in figure 4 was lower than that of the AR-W 7075-T651 Al alloy at lower scattering vectors. Deschamps *et al* [10] and Liu *et al* [11] propose that the scattered intensity is higher due to the larger mean radius of precipitates. The average precipitate radii of 4.00 nm for the wrought as-received 7075-T651 Al alloy is larger than that

of the GISS cast 7075-T6 Al alloy aged at 120°C for 72 h (GISS-PA).

Figure 5 shows the scattering curves for the GISS-cast 7075-T6 aged at 120°C for 72 h (GISS-PA) and wrought 7075-T651 Al alloy, held at 200°C for 1 and 4 h. The average precipitate radius in the wrought alloy clearly increased to 6.41 nm when held for 1 h at 200°C and increased further to 9.75 nm when held for 4 h. In the case of GISS-PA alloy, the precipitate size also increased from 2.50 to 4.32 nm when held at 200°C for 1 h. With the holding time further increased to 4 h, the precipitate size grew to 6.46 nm. These results demonstrate that the precipitates in the microstructure of the wrought alloy are coarser than those in the GISS-PA alloy, at 200°C and that the wrought alloy experiences softening at elevated temperatures [2].

### 3.3 Precipitate coarsening

An increasing average precipitate radius with ageing time is termed a coarsening process. Our measurements of the average precipitate radii show coarsening of the precipitates with ageing that increased with temperature, consistent with the investigation of Du *et al* [2]. The coarsening of Al-Zn-Mg-(Cu) alloys has been well fit with the Lifshitz–Slyozov–Wagner (LSW) model [2,3,10–12]. This model has a linear relationship between particle volume and ageing time ( $t$ ), so that the precipitate radius ( $R$ ) evolves as given below in equation (3)

$$R^3 - R_0^3 = Kt, \quad (3)$$

where  $K$  is the growth co-efficient. Figure 6 shows plots of  $R^3$  vs. ageing time at 120, 145, 165 and 185°C, displaying nearly linear relationships of  $R^3$  to ageing time. The linearity corroborates the LSW model for our observed coarsening process. The growth coefficients determined from the slopes approximately follow a modified Arrhenius type temperature dependency as shown in figure 7. By extrapolation, the

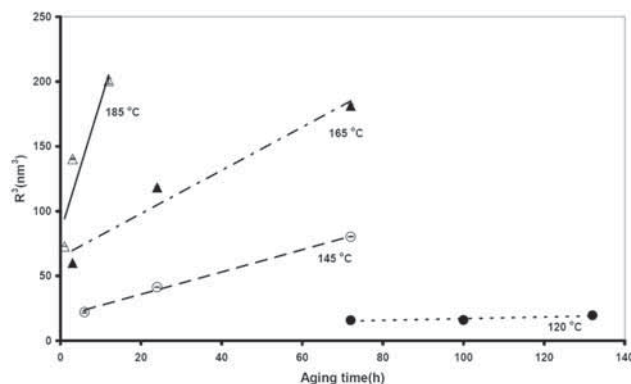


**Figure 6.** Plots of  $R^3$  vs. ageing time for 120, 145, 165 and 185°C show reasonably good fit of linear volume growth models to our data.

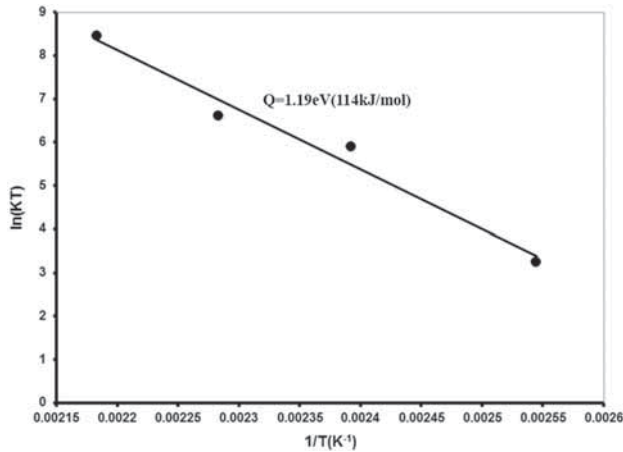


**Figure 7.** A plot  $\ln(KT)$  vs. ageing  $1/T$  is nearly linear displaying a modified Arrhenius type temperature dependency for the coarsening rates.

coarsening rate of precipitates in GISS 7075-T6 Al alloy is expected to increase with the ageing temperature also beyond our experimental range and the rates could be predicted from the approximations fit to our data.

The modified Arrhenius equation for the growth coefficient  $K$  in explicit form is

$$K = \frac{c}{T} \exp\left(\frac{Q}{k_B T}\right), \quad (4)$$

where  $T$  is the ageing temperature and  $c$  is a constant that depends on the precipitate-matrix interfacial energy, the average atomic volume, the equilibrium solute concentration and the solute diffusion coefficient [13]. The theoretical derivation assumes that the changes in concentration and interfacial energy are negligible.

The activation energy  $Q$  in equation (4), for the precipitate coarsening of GISS 7075-T6 Al alloy, was estimated from our data as only 1.19 eV ( $114 \text{ kJ mol}^{-1}$ ), which is close to the 1.22 eV of wrought 7075 Al alloy [2]. This activation energy is within the range 1.17–1.47 eV of activation energies for the diffusion of Cu, Mg and Zn in Al [3,14]. The existence of an  $\eta'$  phase in the specimens aged at 120°C for the peak ageing time and at 145, 165 and 185°C for the onset of hardness plateau time has been known [4]. The current study confirmed that the  $\eta'$  phase coarsens and transforms to the  $\eta$  stable phase by diffusion at long ageing times. The result also suggested that the coarsening mechanism of  $\eta'$  phase is controlled by volume diffusion and there is no interaction among the  $\eta'$  phase particles corresponding to the LSW theory.

In addition, the coarsening dynamics of the GISS 7075-T6 Al alloy appear rather similar to the wrought 7075 Al alloy, based on similar activation energies and precipitate particle sizes determined in the current study. As regards precipitate coarsening at the elevated 200°C temperature, the GISS

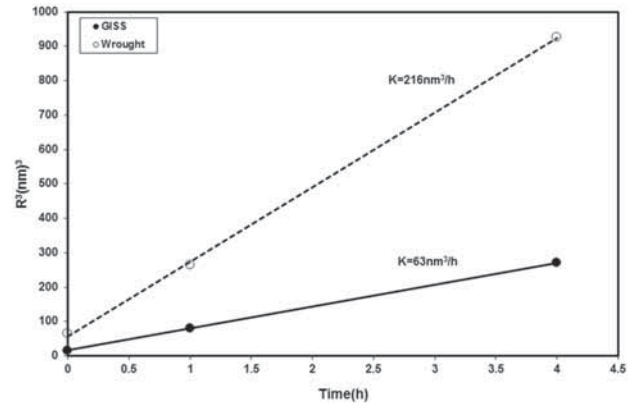


**Figure 8.** Plot  $R^3$  vs. holding time at 200°C for GISS cast 7075-PA (GISS) and wrought 7075 Al alloy (wrought).

7075-PA Al alloy was compared with the wrought 7075-T651 Al alloy.  $R^3$  vs. ageing time at 200°C is plotted for both alloys in figure 8. The precipitate coarsening of both alloys at 200°C is consistent with the LSW theory as the relationship of  $R^3$  and ageing time appears linear. However, the  $63 \text{ nm}^3 \text{ h}^{-1}$  coarsening rate of the GISS 7075-PA Al alloy is about three-fold less than that of the wrought 7075-T651 Al alloy ( $216 \text{ nm}^3 \text{ h}^{-1}$ ). The results imply that the precipitates in the microstructure of the wrought alloy are coarser than those in the GISS-T6 PA alloy, at 200°C, and that the wrought alloy is softened at elevated temperatures [5].

#### 4. Conclusions

The SAXS measurements available at the Siam Photon Laboratory, the SLRI, Thailand, were used to estimate the precipitate particle sizes of the GISS cast 7075-T6 Al alloy. The coarsening of precipitates across ageing temperatures in the range from 120 to 185°C were well fit by an LSW model for times beyond the peak ageing and the onset of hardness plateau. The 1.19 eV activation energy estimated for the studied alloy suggests that the precipitate coarsening is rate limited by diffusion and close to that of wrought 7075 Al alloys. However, the coarsening rate of fine precipitates in the GISS 7075-PA Al alloy is  $63 \text{ nm}^3 \text{ h}^{-1}$  at a temperature of 200°C, which is about three-fold less than that of the wrought 7075-T651 Al alloy ( $216 \text{ nm}^3 \text{ h}^{-1}$ ). This suggests that the GISS sample could be preferable at elevated temperatures.

#### Acknowledgements

This work was financially supported by the Thailand Research Fund (Grant No. MRG5680021) and Prince of Songkla University, Surat Thani Campus (2016). We would like to thank all the staff members of the Siam Photon Laboratory

(beamline No. 1 : SAXS) of the SLRI for their help in conducting the SAXS experiment, and Associate Prof Dr Seppo Karrila for commenting on the manuscript.

## References

- [1] Polmear I J 2006 *Light alloy: from traditional alloys to nanocrystals* (United Kingdom: Butterworth-Heinemann)
- [2] Du Z, Zhou T, Liu P, Li H, Dong B and Chen C 2005 *J. Mater. Sci. Technol.* **21** 479
- [3] Guyot P and Cottignies C 1996 *Acta Mater.* **44** 4161
- [4] Mahathaninwong N, Plookphol T, Wannasin J and Wisutmethangoon S 2012 *Mater. Sci. Eng. A* **532** 91
- [5] Mahathaninwong N, Zhou Y, Babcock S E, Plookphol T, Wannasin J and Wisutmethangoon S 2012 *Mater. Sci. Eng. A* **556** 107
- [6] Glatter O and Kratky O (eds) 1982 *Small angle X-ray scattering* (London. Academic Press)
- [7] Soontaranon S and Rugmai S 2012 *Chin. J. Phys.* **50** 204
- [8] Phinjaroenphan S, Soontaranon S, Chirawatkul P, Chaiprapa J, Busayaporn W, Pongampai S et al 2013 *J. Phys. Conf. Ser.* **425** 1
- [9] SAXSIT Available at: [http://www.slri.or.th/th/index.php?option=com\\_content&view=article&id=276%3Asaxsit-page&catid=55%3Abl13w&Itemid=85](http://www.slri.or.th/th/index.php?option=com_content&view=article&id=276%3Asaxsit-page&catid=55%3Abl13w&Itemid=85)
- [10] Deschamps A, Livet F and Brechet Y 1999 *Acta Mater.* **47** 281
- [11] Liu D, Xiong B, Bian F, Li Z, Li X, Zhang Y et al 2013 *Mater. Sci. Eng. A* **588** 1
- [12] Zheng L J, Chen C O, Bai P C, Zhou T T, Liu P Y and Dong B Z 2003 *Mater. Lett.* **58** 25
- [13] Tsao C S, Lin T L and Yu M S 1999 *J. Alloys Compd.* **289** 81
- [14] Du Z W, Sun Z M, Shao B L, Zhou T T and Chen C Q 2006 *Mater. Charact.* **56** 121